ROUGHNESS INDUCED TRANSITION IN WALL BOUNDED FLOW: A VORTICITY POINT OF VIEW

Saikishan Suryanarayanan and David B. Goldstein
Department of Aerospace Engineering and Engineering Mechanics
The University of Texas at Austin
Austin, Texas 78712, USA
saikishan.suryanarayanan@gmail.com david@ices.utexas.edu

Garry L. Brown
Department of Mechanical and Aerospace Engineering
Princeton University
Princeton, New Jersey 08544, USA
glb1873@msn.com

ABSTRACT

We have recently demonstrated, using experiments and DNS, how boundary layer transition caused by a single discrete roughness element (DRE) can be inhibited by appropriate addition of a discrete roughness element (Sharma et al, 2014; Suryanarayanan et al, 2017a) or distributed roughness (Kuester et al, 2014; Suryanarayanan et al, 2017b). In this paper we explore in greater detail the roughness induced transition (RIT) control via application of a single additional discrete roughness element, and utilize the unique capabilities of our simulation setup to examine the underlying mechanics. Notably we show that for the parameter regimes in which we are interested (Re_{δ}^* ~ 1480, k^+~15; δ^*-boundary layer displacement thickness, k - height of the DRE), we obtain nearly identical results for the boundary layer and for Couette flow, suggesting that the flow evolution is dominated by the near-wall dynamics in case of both the RIT and RIT cancellation cases. Analysis of the evolution of different vorticity components and the associated analysis of the production and dissipation terms provide insights into the transition process and the roles of different components of vorticity. We thus explain why the control works from a vorticity point of view, complementing the related experimental/CFD work (Berger et al, 2017) that examines some of these results from an instability point of view. Using specially engineered simulations, we also address fundamental questions about the receptivity, the deterministic amplification of the steady vortical perturbations, the apparent 'modal' amplification of unsteady vortical perturbations, the subsequent evolution to a chaotic state, and how viscosity and inlet unsteadiness affect the evolution. The present results show that the investigation of RIT leads to novel control techniques and offers the potential to provide further understanding of the basic transition mechanisms in wall-bounded flow.

INTRODUCTION

Roughness induced transition (RIT) in boundary layers (BL) is a technologically important problem that is of fundamental interest. It can be classified under 'by-pass transition', a terminology that is used to label a wide class of transition scenarios that are not dominated by the linear instability of Tollmien-Schlichting waves. A challenge to understanding, predicting or controlling bypass transition is that it can proceed along any of the several possible paths (as outlined by Morkovin, 1969). The precise path may depend on the nature of the disturbance. In the case of RIT, there is the additional complexity of receptivity (White, 2005) - the detailed interaction between the incoming flow and the roughness element, that can lead to both a steady distortion of the local flow field and to unsteady perturbations via selective amplification of disturbances.

RIT is often responsible for undesirable early transition of the boundary layer over aircraft wings. The roughness could be built-in or environmentally accumulated such as through insect impacts. A series of matched studies involving wind tunnel experiments at Texas A&M and direct numerical simulations (DNS) using an immersed boundary method at The University of Texas at Austin have been carried out with the objective of examining methods to control RIT.

The most recent of these results suggest that RIT caused by a single discrete roughness element (DRE) may be controlled passively, either by using a specially designed second DRE ('anti-roughness') placed downstream of the first (Sharma et al, 2014; Suryanarayanan et al, 2017a) or an appropriate use of distributed roughness (Kuester et al, 2014; Suryanarayanan et al 2017b) to shield the DRE. The delay of transition in both cases has been confirmed in both experiments and CFD. Parametric study suggested that the "anti-roughness" scheme was robust to small changes in Reynolds number and to the location of the second element. This is useful from an application point of view, but the results raise a fundamental question - why in one case is there amplification of the 3D vorticity disturbance to a chaotic turbulent state and in another case, at the same Reynolds number, the ordered vortical perturbation does not amplify but decays?

A preliminary control volume analysis of the use of 'anti-roughness' (such as that presented in Suryanarayanan et al., 2017a) revealed an amplification of the high and low speed streaks through a the 'lift-up effect', consistent with the transient growth literature (beginning with Landalh, 1980). The addition of the 'anti-roughness' appeared to suppress this mechanism. Thus an overall picture of RIT appeared to emerge on the nature of the steady disturbance generated by the DRE, the dominant terms

driving the immediate evolution and the effect of anti-roughness in changing this picture.

Numerous questions remained, however, including the following: (1) What is the role of boundary layer thickness, its associated instability, and viscosity? (2)What is the mechanics of the disturbance vorticity field for the single DRE and for the anti-roughness case? (3) What is the mechanics of the subsequent evolution that leads to transition and enhanced mean wall stress? Clarifying the answer to these fundamental questions may illuminate both the physics of RIT and lead to systematic anti-roughness design principles and other novel control schemes for generalized roughness. Seeking this more holistic understanding of the RIT process has been the objective of the present work.

Studying RIT in boundary layers has the merit of being closer to addressing the technological problem and it offers the possibility of matched experiments that can provide both validation of numerical studies and complementary statistics. The abstraction of this technological problem to the well-posed problem of RIT in Couette flow has some advantages - (1) the linear velocity profile of Couette flow is stable to all linear, normal modes and hence there is no interference/interaction with a T-S like mechanism, (2) unlike the boundary layer which also introduces the BL thickness as a further length scale, RIT in Couette flow has only one length scale, namely the roughness height k (for a given roughness element shape), (3) the spanwise vorticity is uniform everywhere in the base flow, (4) there is no variation of the base flow with x and hence a parallel base flow is exact. As a consequence, it would seem that Couette flow presents a simpler, cleaner problem in which to address fundamental questions on RIT, provided it shares the same near-wall velocity profile and viscosity as the boundary layer. In this paper, we present Couette flow simulation results to complement data from boundary layer simulations. (Some results from the BL simulations are also presented in Suryanarayanan et al, 2017a and Berger et al, 2017.)

COMPUTATIONAL SETUP

The in-house developed solver incorporates immersed boundary forces in the channel flow algorithm of Kim, Moin & Moser (1987). The forces are used to generate roughness elements as well as to alter the outflow from the otherwise streamwise periodic setup to a specified inlet velocity profile. The code was originally presented in Goldstein et al (1993,1995) and has since been used in various studies (most recently Strand, 2010; Sharma et al, 2014; Kuester et al, 2014; Goldstein et al, 2016; Suryanarayanan et al 2017a). Many of them involved favorable comparisons with experiments.

Preliminary studies showed that for boundary layer simulations(Re_δ^* ≈435, $k^+ = u_\tau k/\nu \approx 18$) performed on a 768 x 128 x 192 grid, the flow evolution with both the single DRE case and the anti-roughness case closely agreed with dye visualization in matched experiments in a water tunnel. Suryanarayanan et al (2017a) showed that wall shear stress from boundary layer simulations (on a 1534 x 128 x 384 grid, $Re_\delta^* \approx 1480$, $k^+ \approx 15$) for a variety of configurations favorably agreed with naphthalene shear stress visualization in wind tunnel experiments, including the point of transition and the wedge spread angle for the single DRE case and for the prevention of transition for the anti-roughness case.

RESULTS AND DISCUSSION

We took the view that the path to transition could be broadly divided into three stages (1) a 'receptivity' stage, (2) a deterministic amplification, part of which might be understood from an amplification of a locally steady perturbation field and a part that may involve the amplification of a 'narrow spectrum' of time-dependent fluctuations, and (3) the emergence of 'chaotic' vorticity (a 'broad spectrum' of fluctuations), corresponding to the onset of turbulence.

Receptivity

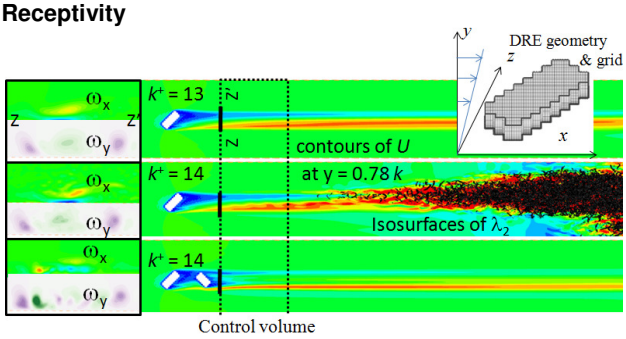

Figure 1. Couette Flow. Right panels: Contours of U at $y = 0.78\,k$ and isosurfaces of λ_2 for the three different cases: single DRE at $k^+ = 13$ and single DRE at $k^+ = 14$ and DRE and anti-roughness element at $k^+ = 14$. Left panels : Contours of ω_x and ω_y in y-ZZ' (x/k=22) planes for the respective cases. Dotted lines show the x-z extents of the control volumes used for vorticity flux analysis in Figs 4 and 8.

Figure 1 plots the flow evolution for three cases - single DRE cases with $k^+ = 14$ and 13 and the anti-roughness case with $k^+ = 14$. The 'base flow' for all three cases described here is Couette flow for reasons given. It can be observed that the near field stage of the flow evolution, up to approximately x/k~20, can be complex in the following ways. The second DRE significantly alters the ω_x and ω_y distributions in a way that cannot perhaps be understood as a simple superposition of the individual effects of the two roughness elements. Furthermore, even a small change in viscosity (or equivalently, a small change in the height of the roughness scaled by the local flow viscous length scale, i.e. from $k^+ = 13$ to 14) can lead to differences in the magnitude of all vorticity components, which significantly alter production terms (Fig.4, to be discussed below).

At this stage it is interesting to note that the perturbations about the base flow, introduced by the case with a single DRE at k^+=14, appear to grow, become unsteady and eventually trigger the transition to turbulence. On the other hand the other two cases, i.e. the anti-roughness case at the same Reynolds number, which introduces perturbations of a similar (or even larger) magnitude but of a different shape, and the single DRE case at the slightly lower Reynolds number, which introduces perturbations of a similar shape and a slightly lower magnitude, do not transition. To seek the explanation for the very different eventual states, we examine the next (second) stage in the evolution.

Amplification of perturbations – Insights from a comparison between BL and Couette flow

To understand the major features of the subsequent evolution, we first carry out a comparison between the flow evolution downstream of the same roughness element for an incoming Blasius boundary layer and for a Couette flow having the same u_τ and viscosity.This would separate the roles of the constant vorticity near wall part of the boundary layer from the outer flow and any possible effect of T-S waves in the boundary layer.

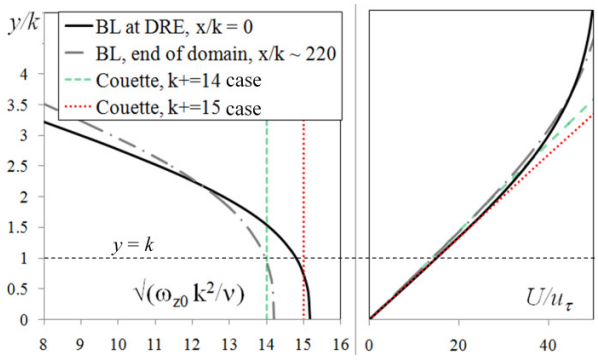

Figure 2. Wall normal variation of ω_z (left) and U (right) in undisturbed Blasius boundary layer and Couette flow.

Figure 2 compares velocity and vorticity profiles of the undisturbed boundary layer at the DRE and at the end of the computational domain considered here, with those in the comparable Couette flow. It can be seen that the variation in vorticity is less than 10% for y < 1.5 k and over the streamwise evolution in the domain (~ 220 k) considered here. This explains the abstraction to an equivalent Couette flow, *if* the T-S instability of the boundary layer does not significantly influence the evolution.

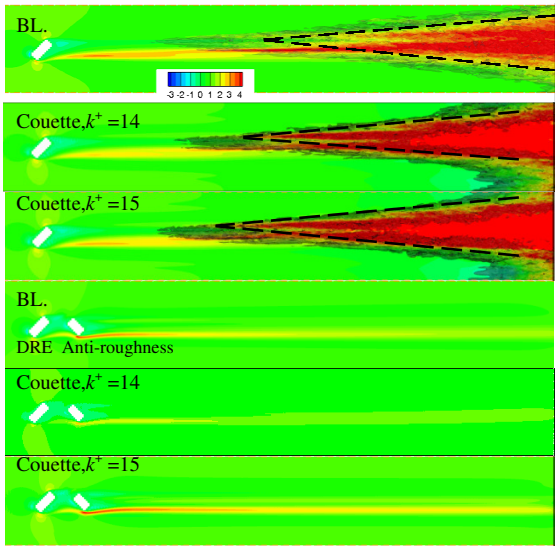

Figure 3. Contours of wall shear stress (red-green) and isosurfaces of turbulence intensity (gray) for single DRE and anti-roughness cases for BL, Couette at k^+=14 and Couette at k^+=15.

Figure 3 compares the time-averaged wall shear stress for the single DRE and anti-roughness cases for boundary layer (k^+ ~ 15) with Couette flows with k^+ = 14 and k^+ = 15. It can be seen that all the single DRE cases transition, leading to a turbulent wedge, a region characterized by both enhanced wall stress and strong unsteadiness. The origin of the wedge and the lateral wedge spread angle do not significantly differ between the boundary layer and the Couette flow cases. The transition process in the spatially developing boundary layer base flow appears to lie between that observed for the k^+=14 and k^+ = 15 Couette flow cases, in terms of parameters such as the origin of the wedge, and is closer to the k^+ = 15 case, as expected from the vorticity profiles. It can also be observed that the addition of the anti-roughness prevents transition (within the computational domain) for both boundary layer and Couette flow.

The overall similarity between RIT in boundary layer and Couette flows is not surprising given the similarity of the vorticity fields in the near field of the roughness. This comparison, however, supports an important conclusion that provided the height of the roughness element is well within the linear velocity profile near the wall of the boundary layer the mechanics of RIT (i.e. amplification of the perturbations introduced by the DRE) has little to do with a coupling with TS modes, since they are entirely absent in the Couette flow cases. (It should be noted, however, that differences between Couette flow and the boundary layer are observed in the spreading of the turbulent wedge in the wall normal direction during the latter stages of transition. Unlike the boundary layer, spanwise vorticity remains constant away from the wall for Couette flow. The turbulent region was observed to grow nearly linearly in y for the Couette flow case. This observation therefore supports the view that the spreading of the chaotic vorticity into the smooth flow occurs by destabilization and entwining of the spanwise vortex lines. This will be analyzed in detail elsewhere, since the present work is focused on the stages of transition that lead to a turbulent wedge rather than the subsequent development of the wedge.)

Mechanics of amplification of vortical perturbations in the uniform vorticity of the base flow

In the previous section it was shown that a given single DRE or combination of DREs introduces a set of vortical perturbations in the base flow (boundary layer or Couette flow). The generation of ω_y can be qualitatively understood by considering the near field to be a kind of 'wake' behind the roughness. The DRE also introduces ω_x, presumably created partly by the tilting of the incoming spanwise vorticity. We find that at say x/k~ 20 the magnitude of time-averaged ω_y is larger than that of ω_x.

While the near field is complex, once perturbations introduced by the DRE are established (stage(1)), can their subsequent downstream development be understood? To begin to answer the question, consider, for the three Couette flow cases analyzed in the previous section, the flux balance for ω_y^2 (see Brown et al, 2015 and Suryanarayanan et al, 2017a for more details) for a control volume beginning just downstream of the element in the near field and ending just upstream of the origin of significant unsteadiness. This control volume ($22<x/k<55$, $0<y/k<11$, $-19.5<z/k<19.5$) is shown in Fig.1. We consider ω_y^2 first since ω_y is substantially larger in magnitude than ω_x.

It can be observed from Fig. 4 that in all three cases the dominant production term is $\iiint \omega_y \omega_z (\partial v/\partial z)$. (Here the spanwise variation of wall normal velocity arises from streamwise vorticity.) This represents the amplification of ω_y by tilting of ω_z and this mechanim is an analog of the Landalh's lift up effect well known to be responsible for transient amplification or algebraic growth of streaks. This term is the largest for the single DRE at $k^+ = 14$ and hence is perhaps the most significant reason for eventually causing transition in this case and not in the other two. Due to the different 'shape' and charactersitic spanwise spacing associated with the vorticity field in the anti-roughness case, the production terms are smaller even though the initial integrated ω_y^2 perturbation *is larger*. As discussed in the introduction, similar conclusions were drawn for RIT in boundary layers by Suryanarayanan et al (2017a). Interestingly, the k^+=13 case does not amplify much, not because dissipation is higher owing to higher viscosity, but because production is lower owing to smaller initial vortical perturbations at the end of the receptivity phase.

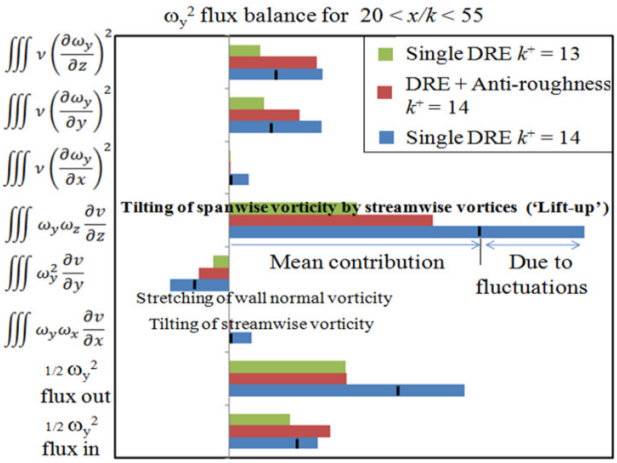

Figure 4. Control volume analysis of sources and dissipation terms of ω_y^2.(All quantities are scaled with wall vorticity of undisturbed flow and k.)

In the analysis presented in Fig. 4, each term (shown in solid colored bars) was computed at different instants of time and *then* averaged. Therefore the production terms describe the origins of the total time-averaged amplification caused by both time-averaged and fluctuating vorticity components. We now repeat the analysis for k^+=14 single DRE case, but this time using the time averaged velocity and vorticity fields to compute the different flux, production and dissipation terms. The respective magnitudes of the different terms thus computed are indicated within the solid blue bars with black dashes. The source terms thus computed therefore represent the amplification due to the mean vorticity field alone. It can be seen that this mean contribution represents the larger fraction of the total amplification. Further, the mean vorticity contribution to the lift-up source term in the single DRE k^+=14 case is still larger than the total lift-up for either of theother two cases.

The contribution made by the fluctuations to the production terms, though not negligible, is counterbalanced by their contribution to dissipation during this phase of the evolution. This therefore raises the question on how crucial is the observed unsteadiness in determing the subsequent evolution.

The role of unsteadiness

The analysis presented so far has focused predominantly on the generation and evolution of steady vorticity perturbations about the base flow. It can be argued that the lift up mechanism that amplifies ω_y does not require an unsteady component. Does unsteady forcing play a critical role, and if so, how can it be understood ?

To begin to answer the question, consider the flow at x/k = 35 for a Couette flow simulation with a single DRE with k^+ = 14. This contains a mean component and a time dependent fluctuation. A simulation was now performed in which only the steady component of the perturbation at x/k = 35 is introduced into the flow. This simulation (see Fig 5), which does not explicitly contain any roughness element within the computational domain, has at the inlet to the computational domain of interest, a time averaged flow field in the y-z plane at x/k = 35 extracted from the simulation *with* the DRE. This input is created by an appropriate set of 'body forces' applied within the buffer zone.

From the results shown in Fig. 5, it can be observed that the simulation with only the steady perturbation **does not** transition, in contrast with the corresponding simulation with the DRE (that had unsteadiness on top of the steady component at x/k =35). Furthermore, even if v and w (and therefore ω_x, the driver of the lift-up) are magnified by a factor of two (not shown here), there is stronger amplification but still the flow **does not** transition. This suggests that the unsteadiness present in the flow at x/k = 35, a location significantly upstream of the origin of the turbulent wedge (at about x/k ~ 70) is crucial for transition.

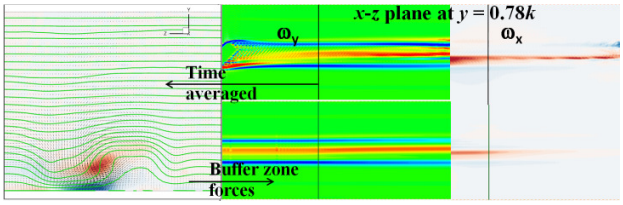

Figure 5. Time averaged slice of data at x/k = 35 (contours of ω_x with isolines of U shown on the left) of Couette flow with a single DRE at k^+ = 14 (top). This data plane is fed in as input into a second simulation without the DRE (bottom). It can be observed that the time averaged input does not lead to transition.

In order to consider this issue, the time traces of the velocity field at different downstream locations along the center plane, are shown in Fig. 6 for Couette flow simulations with k^+ = 14. It can be seen that there is an emergence of what appears to be a single dominant 'modal fluctuation' with a time period of approximately $7\nu/u_\tau^2$ evident at about x/k ~ 15. This is fluctuation is amplified downstream (at x/k = 35), before there is a 'non-linear' development and generation of lower frequencies as witnessed at x/k = 55. A linear T-S instability of the base flow profile is **not** responsible for these observations, since the base flow is Couette flow. Thus, the same underlying mechanics is likely to be responsible for the broadly similar features we observe in the BL case, which we now use for a more detailed analysis because of

the availability of higher resolution simulations than have been obtained to date for Couette flow.

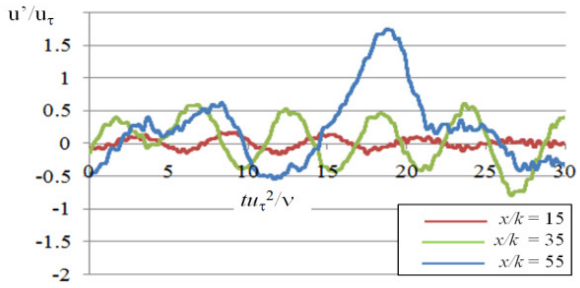

Figure 6. Time traces for streamwise velocity at different downstream locations (z/k = 0, y/k =0.78).

Vorticity dynamics - explanation of the structure and amplification of the unsteady perturbations

Figure 7 illustrates the instantaneous evolution of ω_x and ω_z, along with vortex lines and λ_2 isosurfaces, from the high resolution simulation of the boundary layer with the single DRE. As discussed earlier, the receptivity from the DRE generates ω_y through the lift up of vortex lines as can be seen at x/k=15 in Fig.7. These vortex lines form three dimensional vortical structures which can be seen to undergo a 'modal' amplification (instability) whose passage is responsible for the quasi-periodic fluctuations observed in Fig.6. When viewed in an x-y plane near the centerline, the ω_z fluctuations appear qualitatively similar to what might be observed for a K-H instability associated with a plane shear layer but here, of course, the spanwise extent is very limited.The wavelength of these unsteady perturbations (~ 10 k) is about 10 times the thickness of the shear layer (O(k)), further supporting a qualitatitive connection with K-H. The vortex-lines, however, show that it is an essentially three-dimensional structure and that the distribution of ω_z is directly connected with the positive and negative fluctuations in ω_x. The head of each 'hairpin' in the vortex lines (all have the same sign of spanwise vorticity) tends to 'clump' together as a structure, (as a consequence of the Biot Savart interaction) and this clumping causes (through Biot Savart) the respective legs (ω_y) to bend either forward and backward (as can be seen in the figure), generating a perturbation ω_x. Control volume analysis of the flux of ω^2_x (Fig. 8, for Couette flow) shows that this mechanism is responsible for the magnification of ω^2_x, i.e. $\iiint \omega_x\, \omega_y \partial u/\partial y$ is shown to be the dominant source term. Generation of this unsteady ω_x, causes further unsteady perturbations to ω_y and ω_z, which initially drives a self-amplification process for this modal structure that, when sufficiently large,can be seen to lead to a stage (3) of chaotic vorticity fluctuations. While it may be found that some of these results are specific to the DRE geometry considered here, there is some indication that some of the ideas and mechanisms are of general applicability. For example, Fig.9 shows the contours of fluctuating ω_x for three different Couette flow cases –(1) the base single DRE transitioning case, (2) an initial transient (in time, that eventually dies out) from the non-transitioning anti-roughness case, and (3) a very high amplitude steadily forced case that transitions, but through a quite different steady flow field.

It can be seen that in all cases there is an approximate correspondence with the wavelength and shape of the fluctuation observed for the BL with a single DRE. This provides encouragement for the possibility that the same kind of explanation unravelled for the single DRE case might hold more generally. While further investigation is required to test the generality of the ideas developed in this paper, if true, they provide several novel avenues to control RIT. For example, if the mean ω_x is suppressed, it would prevent the amplification of mean ω_y, which in turn is necessary for the growth of the fluctuations. Some of these cancellation mechanisms occur in the anti-roughness case presented here (and in Suryanarayanan et al, 2007a), and in distributed roughness shielding (Suryanarayanan et al, 2007b), and they suggest additional methods of RIT control such as a local disruption of temporal fluctuations (Fig. 5).

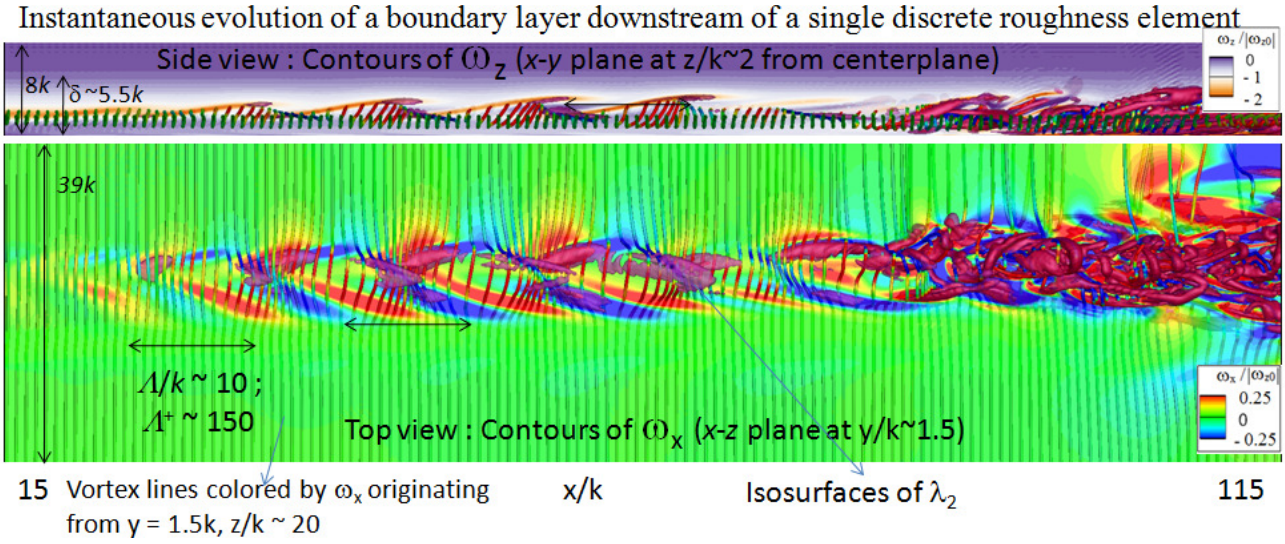

Figure 7. Dynamics of (instantaneous total) ω_x, ω_z and vortex lines in Boundary layer with k^+ = 15

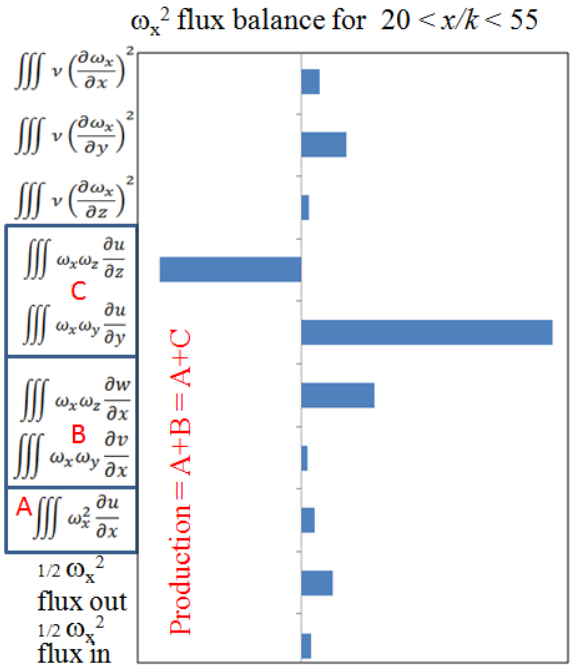

Figure 8. Analysis of sources and dissipation terms of ω_x^2 for Couette flow with single DRE (k^+ = 14) in a control volume defined by 22<x/k<55, 0.4<y/k<11, -19.5<z/k<19.5.

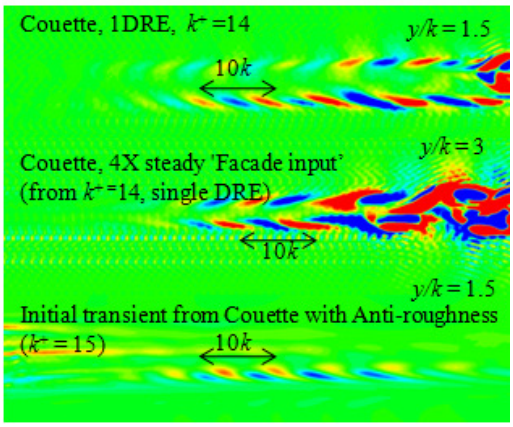

Figure 9. Contours of perturbation ω_x (time average subtracted from instantaneous value) in a y-z plane for different Couette flow cases. Note that the wavelength of the perturbation roughly corresponds to the length of the double arrow that indicates a length of 10k, the wavelength observed for BL in Fig.7.

ACKNOWLEDGEMENTS

This work is supported by the Air Force Office of Scientific Research under grant #FA9550-15-1-0345.

REFERENCES

Berger, A.R., McMillan, M., White, E.B, Suryanarayanan, S, and Goldstein, D.B.., 2017, "Suppression of Transition Behind a Discrete Roughness Element Using a Downstream Element", *Tenth International Symposium on Turbulence and Shear Flow Phenomena* (TSFP10), July 6-9, 2017, Chicago-IL, USA

Landahl, M. T., 1980, "A note on an algebraic instability of inviscid parallel shear flows." *J.Fluid Mech.*Vol. 98 No. 2, pp: 243-251.

Goldstein, D., Chu, J., & Brown, G., 2017,"Lateral Spreading Mechanism of a Turbulent Spot and a Turbulent Wedge. Flow", *Turbulence and Combustion*, Vol. 98 No.1, pp. 21-35.

Goldstein, D.B., Handler, R., and Sirovich, L., 1993,"Modeling a no-slip flow boundary with an external force field," *J. Comp. Phys*., Vol. 105, pp. 354-366.

Goldstein, D. B. , Handler, R. A. and Sirovich, L. , "Direct numerical simulation of turbulent flow over a modeled riblet covered surface," *J. Fluid Mech*., Vol. 302, 1995, pp. 333-376.

Kim, J., Moin, P. and Moser, R.,1987, "Turbulence statistics in fully developed channel flow at low Reynolds number", *J.Fluid Mech.*, Vol. 177, pp.133-166.

Kuester, M. S., Sharma, A., White, E. B., Goldstein, D. B., & Brown, G.L, 2014, "Distributed Roughness Shielding in a Blasius Boundary Layer", *AIAA* Paper 2014-2888.

Morkovin, M.V.,1969, "Critical evaluation of transition from laminar to turbulent shear layers with emphasis on hypersonic traveling bodies", AFRL Report AFF DL–TR–68–149.

Sharma, A., Drews, S. D., Kuester, M. S., Goldstein, D. B., and White, E. B., 2014, "Evolution of Disturbance due to Discrete and Distributed Surface Roughness in Initially Laminar Boundary Layers," *AIAA* Paper 2014-0235.

Strand, J. and Goldstein, D.B.,2010, "Application of passive surface textures to control the growth of turbulent spots at moderately high Reynolds numbers". *Int. J. of Flow Control*. Vol. 2, No. 2.

Suryanarayanan, S., Goldstein, D.B., Brown, G.L., Berger, A.R. and White, E.B., 2017a, "On the Mechanics and Control of Boundary Layer Transition induced by Discrete Roughness Elements", AIAA 2017-0307, In *proceedings of 55th AIAA Aerospace Sciences Meeting,* 9 - 13 January 2017, Grapevine, Texas, USA.

Suryanarayanan, S., Goldstein, D.B., Berger, A.R., White, E.B., and Brown, G.L., 2017b, " Mechanics of Distributed Roughness Shielding,", abstract accepted for 2017 *AIAA Aviation Forum and Exposition*, 5–9 June 2017, Denver, Colorado, USA.

White, E.B., Rice, J.M. and Ergin, F.G.,2005, "Receptivity of stationary transient disturbances to surface roughness", *Physics of Fluids*, Vol. 17, No.6, pp.064109.